On Nonobtuse Refinements of Tetrahedral Finite Element Meshes

Sergey Korotov
BCAM – Basque Center for Applied Mathematics
Alameda de Mazarredo 14, E–48009 Bilbao, Spain
IKERBASQUE, Basque Foundation for Science
E–48011 Bilbao, Spain
korotov@bcamath.org

Abstract

It is known that piecewise linear continuous finite element (FE) approximations on nonobtuse tetrahedral FE meshes guarantee the validity of discrete analogues of various maximum principles for a wide class of elliptic problems of the second order. Such analogues are often called discrete maximum principles (or DMPs in short). In this work we present several global and local refinement techniques which produce nonobtuse conforming (i.e. face-to-face) tetrahedral partitions of polyhedral domains. These techniques can be used in order to compute more accurate FE approximations (on finer and/or adapted tetrahedral meshes) still satisfying DMPs.

Keywords: Discrete maximum principle, Nonobtuse tetrahedral refinement, Finite element method.

1. Introduction: maximum principles

The maximum principles (i.e. a priori estimation of the unknown solution via given data) represent the most basic properties of (classical) solutions of the second order elliptic problems [17]. In this paper we survey some of our results on their discrete analogues – discrete maximum principles (DMPs) for $3d$ nonlinear elliptic boundary-value problems solved by linear tetrahedral finite elements (FEs). The present work generalizes our earlier paper [8] in several respects - thus, we also survey some recently developed algorithms for local (around edges and near faces/interfaces) conforming refinements of the meshes preserving the nonobtuseness property, which is a sufficient condition guaranteeing the validity of DMPs.

Linear tetrahedral finite elements are very popular for solving various problems described by partial differential equations (PDEs), especially if a high

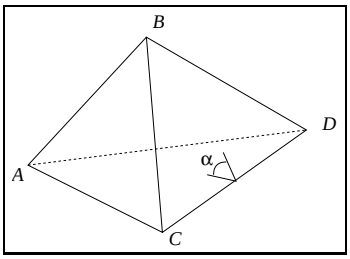

Figure 1: Tetrahedron $ABCD$ whose faces ACD and BCD form the angle α.

regularity of the corresponding solutions cannot be guaranteed (e.g. in the case of complicated geometries). The structure and properties of the associated FE matrix strongly depend on the dihedral angles between faces of tetrahedral elements. To demonstrate this, let us consider an arbitrary tetrahedron $ABCD$ (see Fig. 1). Let ϕ_i and ϕ_j be two linear functions such that

$$\phi_i(A) = 1,\ \phi_i(B) = \phi_i(C) = \phi_i(D) = 0,$$

$$\phi_j(B) = 1,\ \phi_j(A) = \phi_j(C) = \phi_j(D) = 0.$$

Then a straightforward calculation leads to the following formula (see [15])

$$\nabla\phi_i \cdot \nabla\phi_j = -\frac{\mathrm{meas}_2 ACD\, \mathrm{meas}_2 BCD}{9\,(\mathrm{meas}_3 ABCD)^2} \cos\alpha, \tag{1}$$

where α is an angle between the faces ACD and BCD, and the symbol meas_d stands for d-dimensional measure (i.e. the area of a triangle for $d = 2$ and the volume of a tetrahedron for $d = 3$). Thus, each obtuse dihedral angle of the tetrahedron $ABCD$ gives a positive contribution to the corresponding off-diagonal entry of the element FE matrix e.g. when solving a boundary value problem with the Laplace operator by FEM.

Note that the same observation holds (see [15, 5]) for a wider class of nonlinear elliptic problems of the form

$$-\mathrm{div}(b(x, u, \nabla u)\nabla u) = f(x) \quad \text{in} \quad \Omega, \tag{2}$$

$$u = 0 \qquad \text{on} \quad \partial\Omega, \tag{3}$$

where $b(\cdot,\cdot,\cdot)$ is some positive smooth function. Here and in what follows Ω is a bounded polyhedral domain with Lipschitz boundary $\partial\Omega$. Equation (2) is used for modelling many phenomena in real-life applications, see [5] for some examples.

For problem (2)–(3) the most popular *maximum principle* reads as follows (cf. [17])

$$f(x) \le 0 \quad \text{in} \quad \overline{\Omega} \qquad \Longrightarrow \qquad \max_{x\in\overline{\Omega}} u(x) \le 0. \tag{4}$$

It is thus natural to look for a class of finite elements such that a similar implication (i.e. DMP) is guaranteed for the corresponding FE approximations a priori. In our case it means that (cf. [3])

$$f(x) \le 0 \quad \text{in} \quad \overline{\Omega} \qquad \Longrightarrow \qquad \max_{x \in \overline{\Omega}} u_h(x) \le 0, \tag{5}$$

where u_h is the piecewise linear continuous FE approximation of the solution of (2)–(3). (The definition for the subindex h will be given in the next section.)

2. On nonobtuse tetrahedral FE meshes

Definition 1 *A finite set of tetrahedra is called a tetrahedral FE mesh of $\overline{\Omega}$ if*

i) the union of all the tetrahedra is $\overline{\Omega}$,

ii) the interiors of the tetrahedra are mutually disjoint,

iii) any face of any tetrahedron from the set is either a face of another tetrahedron in the set, or a subset of $\partial\Omega$.

For a given FE mesh $\mathcal{T}_h$ (with elements denoted by the symbol T) the *discretization parameter* h stands for the maximum length of all edges in $\mathcal{T}_h$, i.e.,

$$h = \max_{T \in \mathcal{T}_h} h_T, \quad \text{where} \quad h_T = \operatorname{diam} T.$$

Definition 2 *An infinite sequence $\mathcal{F} = \{\mathcal{T}_h\}_{h \to 0}$ of FE meshes of $\overline{\Omega}$ is called a family of FE meshes if for every $\varepsilon > 0$ there exists $\mathcal{T}_h \in \mathcal{F}$ with $h < \varepsilon$.*

Definition 3 *A tetrahedron is said to be nonobtuse if all its six dihedral angles between the faces are less than or equal to $\pi/2$.*

Definition 4 *A tetrahedral FE mesh is said to be nonobtuse if it contains only nonobtuse tetrahedra.*

By [3], linear triangular nonobtuse finite elements guarantee the validity of DMP (5) for the Poisson equation in $2d$. This result was generalized to $3d$ case in [15], namely, that linear tetrahedral FEs applied to problem (2)–(3) yield approximations satisfying (5) if nonobtuse tetrahedral FE meshes are used. The main ingredient in those works was to provide that resulting FE matrices are monotone. This is the case if they are e.g. Stieltjes ones, in particular, if they have nonpositive off-diagonal entries (see [20] for details). The last condition is obviously guaranteed for nonobtuse tetrahedral meshes due to formula (1).

In order to decrease the discretization error, a given FE mesh should be refined locally and/or globally during the computational process. That is why the issue of preserving the nonobtuseness property while refining the meshes naturally arises.

2.1. Global nonobtuse refinement technique

In this subsection we describe a global refinement algorithm producing nonobtuse tetrahedra only.

Definition 5 *A tetrahedron is said to be a path tetrahedron if it has three mutually perpendicular edges which do not pass through the same vertex.*

The reason for the name of the above defined tetrahedron is due to the fact that its three perpendicular edges form a "path" (see Fig. 2 (left)).

Lemma 1 *Any path tetrahedron is nonobtuse.*

For the proof see [7, p. 728–729].

Theorem 1 *Let T be an arbitrary tetrahedron such that its circumcentre belongs to T, and let all faces of T be nonobtuse triangles. Then there exists a family of tetrahedral FE meshes of T, which contains only path tetrahedra.*

This theorem is proved in [7] and [16].

Note that each path tetrahedron satisfies the assumptions of Theorem 1, since its faces are right triangles and its circumcentre is the midpoint of the longest edge. In Fig. 2 (right) a partition of a tetrahedron T, that satisfies the assumptions of Theorem 1, into path tetrahedra, is sketched. Such a partition is defined in the following way. First we divide each face F of T into 6 or 4 right subtriangles by connecting the circumcentre of F with 3 vertices and 3 midpoints of sides of F. The common vertex of these subtriangles is the circumcentre of F. This kind of plane refinement we call *2d yellow*. Denoting the circumcentre of T by G, we can define the path subtetrahedra as convex hulls of G and particular right subtriangles on the surface of T. We call such a three-dimensional refinement as the *3d yellow*.

It is clear that a common face F of any two adjacent tetrahedra (satisfying the assumptions of Theorem 1) in a given mesh is divided by the above technique in a unique way. Therefore, we can formulate the main result of this subsection as follows.

Theorem 2 *Let the initial FE mesh of $\overline{\Omega}$ be such that for any tetrahedron T its circumcentre belongs to T, and let all faces of all T be nonobtuse triangles. Then there exists a family of tetrahedral FE meshes of $\overline{\Omega}$ containing only path tetrahedra.*

2.2. Local nonobtuse refinement techniques

Towards a vertex: The key idea of local refinement technique producing only nonobtuse tetrahedra in the face-to-face manner towards some vertex is exposed in the following theorem.

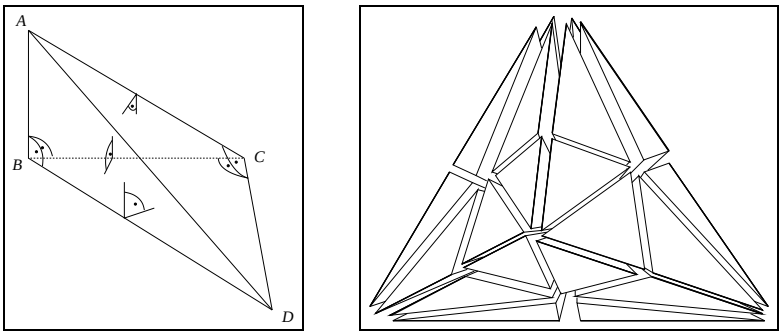

Figure 2: A path tetrahedron $ABCD$, whose edges AB, BC, and CD form a "path", all its right angles (within faces and dihedral ones) are indicated (left). $3d$ yellow partition of a tetrahedron into path subtetrahedra (right).

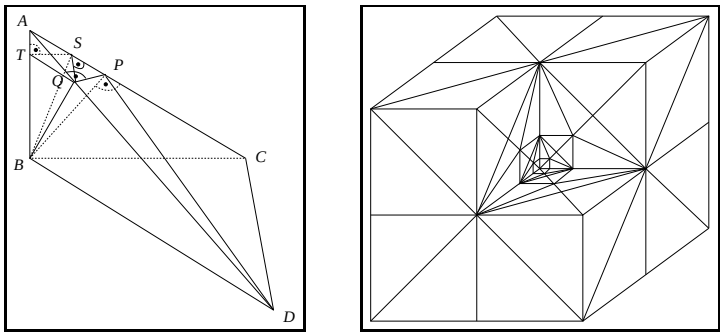

Figure 3: Partition of a path tetrahedron $ABCD$ into 5 path subtetrahedra (left). Local refinement into nonobtuse tetrahedra near Fichera corner (right).

Theorem 3 *Let $ABCD$ be a path tetrahedron whose edges AB, BC, and CD are mutually perpendicular. Then there exists an infinite sequence of nonobtuse tetrahedral FE meshes of $ABCD$ consisting of path tetrahedra only that locally refine towards the vertex A.*

For a detailed constructive proof see [9]. Its main idea is sketched in Fig. 3 (left). Using several appropriate orthogonal projections, we first subdivide the tetrahedron $ABCD$ into five nonobtuse tetrahedra. Then we show that the path tetrahedron $ATSQ$ from Fig. 3 (left) is similar to the original tetrahedron $ABCD$. The subtetrahedron $ATSQ$ can be now decomposed into 5 subtetrahedra in a similar way as $ABCD$. In this manner, we obtain recursively the required infinite sequence of nonobtuse tetrahedral FE meshes condensing towards the point A.

The above idea can be used e.g. for local refinements a polyhedral domain $\Omega = (-1,1)^3 \setminus [0,1)^3$ which is the union of 7 cubes, see Fig. 3 (right). Each cube is first divided in a standard way into 6 path tetrahedra having a common

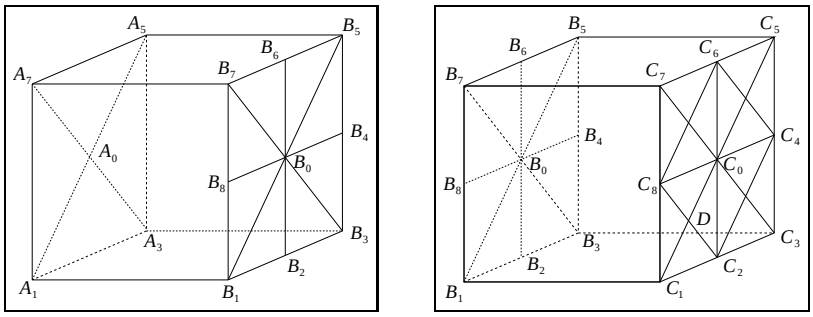

Figure 4: Partition of two adjacent square prisms into nonobtuse tetrahedra.

vertex in the reentrant corner of Ω. For each of the $7 \times 6 = 42$ tetrahedra we apply the algorithm given by Theorem 3 such that the partition of each path tetrahedron is just the mirror image of the partition of any adjacent tetrahedron having a common face. Note that the concave (also named reentrant) corner in Fig. 3 (right) is often called the *Fichera corner*. See [9] for similar handling some Fichera-like corners.

Near a face/interface: Here, we present the key from our recent work [10] (see Fig. 4 and 5) on nonobtuse tetrahedral refinements towards a flat face/interface of the solution domain. For this purpose we take a square prism and its adjacent square prism. Denote their vertices and some other nodes as sketched in Fig. 4, where also partitions of some faces are given.

In what follows, let $s = |B_1B_3| = |B_3B_5|$ denote the lengths of the edges of the square faces of the prisms, and let $l_1 = |A_0B_0|$ and $l_2 = |B_0C_0|$ be their thicknesses. First, we decompose the left square prism $A_1A_3A_5A_7B_1B_3B_5B_7$ of Fig. 4 into four triangular prisms whose common edge is A_0B_0. Second, we decompose each triangular prism into four tetrahedra. For instance, the triangular prism $A_0A_1A_3B_0B_1B_3$ will be divided in the following way (see Fig. 5):

$A_0A_1A_3B_0$, $A_1B_1B_2B_0$ (path tetrahedron),
$A_3B_3B_2B_0$ (path tetrahedron), and $A_1A_3B_0B_2$.

The first three resulting tetrahedra are clearly nonobtuse. The last tetrahedron $A_1A_3B_0B_2$ is nonobtuse if and only if

$$|B_1B_3| \le 2|A_0B_0|, \quad \text{i.e.} \quad l_1 \ge \frac{s}{2}. \tag{6}$$

The other three triangular prisms, $A_0A_3A_5B_0B_3B_5$, $A_0A_5A_7B_0B_5B_7$, and $A_0A_1A_7B_0B_1B_7$, can be subdivided similarly.

Next, we decompose the right adjacent square prisms $B_1B_3B_5B_7C_1C_3C_5C_7$ of Fig. 4 into eight triangular prisms whose common edge is B_0C_0. Further, e.g. the triangular prism $B_0B_1B_2C_0C_1C_2$ will be divided into four tetrahedra like in the previous step:

$B_0B_1B_2C_2$ (nonobtuse tetrahedron), $B_0C_0DC_2$ (path tetrahedron),

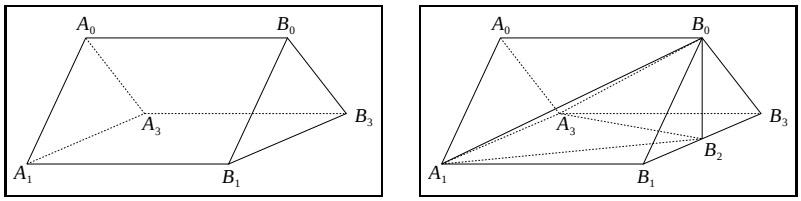

Figure 5: Decomposition of a prism $A_0A_1A_3B_0B_1B_3$ into 4 tetrahedra.

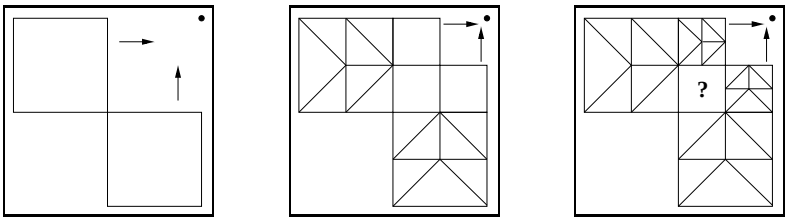

Figure 6: Several refinements towards the vertical edge (marked by the bold dot, view from the top). The problematic zone is marked by the question mark.

$B_1C_1DC_2$ (path tetrahedron), and $B_0B_1DC_2$.

The last tetrahedron is nonobtuse provided

$$|B_0B_1| \leq 2|B_0C_0|, \quad \text{i.e.} \quad l_2 \geq \frac{\sqrt{2}s}{4}. \tag{7}$$

This condition is necessary and sufficient to guarantee a nonobtuse decomposition of the triangular prism $B_0B_1B_2C_0C_1C_2$ into four nonobtuse tetrahedra as described above.

The other seven triangular prisms can be divided into nonobtuse tetrahedra similarly. In this way (i.e., under conditions (6) and (7)) we get a face-to-face nonobtuse partition of two adjacent square prisms. The left square prism of Fig. 4 is subdivided into 16 and the right prism into 32 nonobtuse tetrahedra. This enables us to form layers and use this process repeatedly towards faces/interfaces (see [10] for some practical examples).

Around an edge: Here, the recent algorithm from [11] is sketched. In the construction of the previous case (about refinements near face/interface), we take both prisms be of the thickness $\frac{d}{2}$, i.e. $l_1 = l_2 = \frac{d}{2}$. Therefore, two square prisms in Fig. 4 form a cube with edges of the length d.

In Figure 6, we observe several principal refinement steps towards the chosen vertical edge in the upper right corner (view from the top). The advancing (according to arrows) blocks with the shown refinement of their upper faces are always treated as in Fig. 4 and 5 (with their "own" $l_1 = l_2 = \frac{d}{2}$). The problematic zone (marked by the question sign) and its refinement which provide the conformity with the "surroundings" will be discussed further. It is enough to consider a few first steps only (as in Fig. 6), since the situation repeats up to

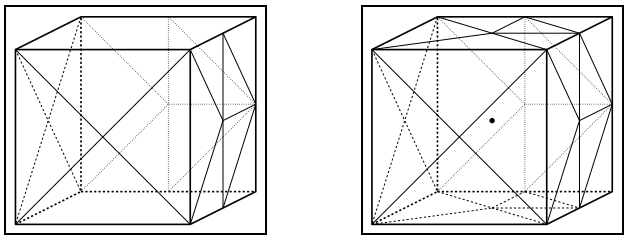

Figure 7: Refinement of one of the two cubes in the problematic zone, only forced "face refinement" lines (due to the conformity requirements) are sketched (left). Full "face refinement" of the left cube (the bold dot is its center) (right).

scaling. In what follows, we always consider only the upper layer (of the width d) from the initial mesh, since the (possible) other layers (under it, each of the width d, too) can be treated similarly using symmetry argument.

The zone marked by the question mark in Fig. 6 is, in fact, made of two cubes (one above the other) of the size $\frac{d}{2} \times \frac{d}{2} \times \frac{d}{2}$ each. It is enough to show how to partition, conformly with the surroundings, the upper cube, since the lower cube can be partitioned using the mirror reflection via their common face. The method for this purpose is illustrated in Fig. 7 and 8. First, in Fig. 7 (left) we sketch those faces whose refinement stencils are dictated by the previous constructions, and further, as illustrated in Fig. 7 (right) we partition the cube into nonobtuse tetrahedra taking convex hulls of the center of the cube and the marked right triangles on the faces, besides the upper and lower right subcubes, which we split in a special way (into 5 nonobtuse teterahedra each) as demonstrated in Figure 8.

We notice that we can do infinitely many steps in the total above construction with the choice $l_1 = l_2 = \frac{d}{2}$ and the overall conformity of any resulting meshes, obviously moving towards the chosen edge, is guaranteed.

In real-life calculations we perform only a finite number of refinements. Therefore, we have to divide the "remaining" zone around the edge, whose position is illustrated by the black dot in Fig. 6. Each subcube in that zone has to be divided so that it fits to the triangulation of the right face of the right cube from Fig. 4 (right). We could apply for this purpose e.g. the division into 24 cube corner tetrahedra as sketched in Fig. 8 (right). A direct calculation shows that the above algorithm applied to a cube produces, in terms of Fig. 6 (from the left to the right) conforming nonobtuse tetrahedral meshes with 640, 1536, and 3328 elements, respectively.

3. Concluding remarks

Remark 1 Nonobtuseness of tetrahedral FE meshes represents only a sufficient condition to guarantee DMP. In [12] we present a weakened DMP-condition on the shape of tetrahedra, which enables us to use also some tetrahedra with

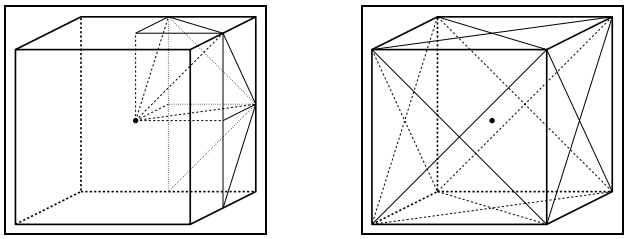

Figure 8: Refinement of one of the two sub-cubes into 5 nonobtuse tetrahedra (left). Partition of a cube into 24 cube corner tetrahedra. They are defined as the convex hull of the centre of the cube and a particular triangle on the surface (right).

dihedral angles slightly bigger than $\pi/2$.

Remark 2 If we consider a more general elliptic problems with lower-order terms [5], DMP would be guaranteed on acute tetrahedral FE meshes only, i.e. on those meshes whose elements are acute tetraheda (with acute dihedral angles). However, the problem of partitioning into acute tetrahedra is more hard than that one in the case of nonobtuse ones. Available results in this direction are reported in works [1, 2, 6, 14, 18, 19].

Remark 3 DMPs can also be used for proving the convergence of FE approximations in the maximum norm [3].

Remark 4 More sophisticated forms of maximum principles (on continuous and discrete levels) are presented e.g. in [5] – for boundary conditions different from the zero Dirichlet one (3), and in [4] – for the case f from (2) is arbitrary.

Remark 5 Nonobtuse tetrahedra satisfy the so-called maximum angle condition (see [13]), which is commonly used for convergence proofs in the FE analysis.

Acknowledgement: This paper was supported by Grant MTM2011-24766 of the MICINN, Spain.

References

[1] J. Brandts, S. Korotov, M. Křížek & J. Šolc, On nonobtuse simplicial partitions, *SIAM Rev.* 51 (2009), 317–335.

[2] D. Eppstein, J. M. Sullivan & A. Üngör, Tiling space and slabs with acute tetrahedra, *Comput. Geom.: Theory and Appl.* 27 (2004), 237–255.

[3] P. G. Ciarlet & P.-A. Raviart, Maximum principle and uniform convergence for the finite element method, *Comput. Methods Appl. Mech. Engrg.* 2 (1973), 17–31.

[4] I. Faragó, S. Korotov & T. Szabó, On modifications of continuous and discrete maximum principles for reaction-diffusion problems, *Adv. Appl. Math. Mech.* 3 (2011), 109–120.

[5] J. Karátson & S. Korotov, Discrete maximum principles for finite element solutions of nonlinear elliptic problems with mixed boundary conditions, *Numer. Math.* 99 (2005), 669–698.

[6] E. Kopczyński, I. Pak & P. Przytycki, Acute triangulations of polyhedra and the Euclidean space, in *Proc. of the Annual Sympos. on Comput. Geom.,* Snowbird, Utah, 2010, 307–313.

[7] S. Korotov & M. Křížek, Acute type refinements of tetrahedral partitions of polyhedral domains, *SIAM J. Numer. Anal.* 39 (2001), 724–733.

[8] S. Korotov & M. Křížek, *Discrete maximum principle in the finite element modelling.* In "Proceedings of The Fifth European Conference on Numerical Mathematics and Advanced Applications (ENUMATH–2003), Prague, Czech Republic" (ed. by M. Feistauer et al.), Springer-Verlag, 2004, 580–586.

[9] S. Korotov & M. Křížek, Global and local refinement techniques yielding nonobtuse tetrahedral partitions, *Comput. Math. Appl.* 50 (2005), 1105–1113.

[10] S. Korotov & M. Křížek, Nonobtuse local tetrahedral refinements towards a polygonal face/interface, *Appl. Math. Lett.* 24 (2011), 817–821.

[11] S. Korotov & M. Křížek, Local nonobtuse tetrahedral refinement around an edge, *Appl. Math. Comput.*, 219 (2013), 7236–7240.

[12] S. Korotov, M. Křížek & P. Neittaanmäki, Weakened acute type condition for tetrahedral triangulations and the discrete maximum principle, *Math. Comp.* 70 (2001), 107–119.

[13] M. Křížek, On the maximum angle condition for linear tetrahedral elements, *SIAM J. Numer. Anal.* 29 (1992), 513–520.

[14] M. Křížek, There is no face-to-face partition of R^5 into acute simplices, *Discrete Comput. Geom.* 36 (2006), 381–390, Erratum 44 (2010), 484–485.

[15] M. Křížek & Q. Lin, On diagonal dominance of stiffness matrices in 3D, *East-West J. Numer. Math.* 3 (1995), 59–69.

[16] M. Křížek & J. Pradlová, Nonobtuse tetrahedral partitions, *Numer. Methods Partial Differential Equations* 16 (2000), 327–334.

[17] M. H. Protter & H. F. Weinberger, *Maximum Principles in Differential Equations*, Prentice-Hall, New Jersey, 1967.

[18] A. Üngör, Tiling 3D Euclidean space with acute tetrahedra, in *Proc. Canadian Conf. Comput. Geom., Waterloo,* 2001, 169–172.

[19] E. VanderZee, A. N. Hirani, V. Zharnitsky & D. Guoy, A dihedral acute triangulation of the cube, *Comput. Geom.* 43 (2010), 445–452.

[20] R. S. Varga, *Matrix Iterative Analysis*, Prentice-Hall, New Jersey, 1992.